

Large domain walls near crack lines in ferrimagnetic garnet films

L. E. Helseth,^{1,2} M. Kurniawan,² R. W. Hansen,³ and T. H. Johansen³

¹*Department of Physics and Technology, University of Bergen, N-5007 Bergen, Norway*

²*Division of Physics and Applied Physics, School of Physical and Mathematical Sciences, Nanyang Technological University, Singapore 639798, Singapore*

³*Department of Physics, University of Oslo, NO-0317 Oslo, Norway*

(Received 6 November 2007; revised manuscript received 18 January 2008; published 29 February 2008)

We investigate the structure of domain walls near cracks in crystalline magnetic garnet films with in-plane anisotropy using magnetization measurements combined with spatially resolved magneto-optic imaging. It is found that the magnetization vector has a component perpendicular to the film near the crack, but rotates to align with the film a few micrometers away. The domain walls are extraordinary large, with an extension of typically 10 μm , and are found to have opposite polarity on each side of the crack.

DOI: [10.1103/PhysRevB.77.064433](https://doi.org/10.1103/PhysRevB.77.064433)

PACS number(s): 75.70.Kw, 75.60.Ch

I. INTRODUCTION

Bismuth-substituted iron garnet films are known to have a giant magneto-optical response, which together with their low coercivity make them very attractive as magnetic sensors.¹ During the last decades, the main efforts have been directed toward optimizing growth^{2–5} and characterization^{6–10} of these films for probing small magnetic fields, visualize flux distributions in superconductors, and other magnetic structures.^{11–14} More recent studies have demonstrated that light can induce magnetic structures in these films,¹⁵ thus proving their usefulness for studying a wide variety of optical and magnetic phenomena.

Magnetic crystalline films are often grown on substrates. Cracks are commonly formed in the magnetic films when there is a mismatch between the lattice parameters of the substrate and the growing film. Mechanical stress σ alters the uniaxial anisotropy constant K_u according to $K_u = K_{u0} + (3/2)\sigma\lambda$, where K_{u0} is the uniaxial anisotropy constant in the absence of stress and λ is a magnetostrictive coefficient ($\lambda \sim -10^{-5}$ for the garnet films).¹⁶ The modulation in anisotropy may introduce distinct domain and domain wall structures.¹⁷ Recently, it was demonstrated that cracks in bismuth-substituted magnetic garnet films result in characteristic domain wall structures which can be used to efficiently trap and manipulate magnetic colloids, thus allowing one to use the cracked magnetic films for micro- and nanomanipulation in microfluidic settings as well as for investigating diffusion and forces in low-dimensional systems.^{18–21} However, the micromagnetic behavior of these domain walls is far from understood, and further research is needed to gain better insight in their micromagnetic properties.

Here, we study the domain wall structure near cracks in ferrimagnetic garnet films and show that the magnetization has a vector component perpendicular to the film near the crack, but rotates to align with the film about ten micrometers away. This behavior is attributed to the pinning of the magnetic moment due to stress-induced anisotropy, and we use a micromagnetic model to obtain further insight into the rotation of the magnetization vector. Although domains and domain walls near localized stress patterns and boundaries have been studied in other types of magnetic films (see, e.g.,

Refs. 22 and 23 and references therein), we are not aware of such studies of domain walls near crack lines in garnet films. Given the potential of these films in magneto-optic imaging and microfluidic systems, it is therefore of interest to be able to understand such structures in more detail.

II. EXPERIMENT

Single crystal ferrite garnet films were grown by isothermal liquid phase epitaxy onto a 0.5 mm (100) oriented gadolinium gallium garnet substrates as previously reported.^{3,7,8} In such garnet films, if synthesized under proper conditions, the magnetization vector will have an in-plane orientation. By controlling the amount of bismuth and gallium such that the lattice mismatch (i.e., the relative difference between the lattice parameters) between the magnetic film and the substrate is larger than 10%, we obtained a partially cracked ferrite garnet film of composition $\text{Lu}_{2.5}\text{Bi}_{0.5}\text{Fe}_{4.9}\text{Ga}_{0.1}\text{O}_{12}$. The cracks form an intricate network running along the crystallographic axes, as seen in Fig. 1(a), and near these lines, characteristic magnetic domain walls form. The cracks are typically a few nanometers wide and form straight line segments with length ranging from 100 μm to more than 1 mm. The ferrite garnet film exhibits a large Faraday rotation, which allows one to visualize its domain structure using a polarization microscope (Leica DMLP) in transmission mode equipped with a digital charge coupled device (CCD) camera. Upon imaging the corresponding domain wall structure using the polarization micro-

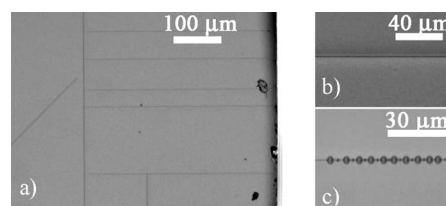


FIG. 1. (a) A magnetic film grown on a mismatched substrate has a number of cracks, (b) each of which induces a domain wall structure in the garnet film (c) which can be used to trap different kinds of magnetic colloids.



FIG. 2. AFM image of a crack in the garnet film.

scope, we observe the structure seen in Fig. 1(b). Such domain wall structures can be used to trap a number of different magnetic colloids. In Fig. 1(c), it is demonstrated how this domain wall structure can be used to trap paramagnetic spheres with diameters of 2.8 and 1.0 μm (see also Ref. 18). Figure 2 shows an atomic force microscopy (AFM) image of one of the cracks in the garnet film. It is seen that the typical width of the crack is less than 100 nm, whereas its length can be several millimeters. The crack is believed to extend through the thickness of the film, but our AFM study did not help resolve this issue due to the finite height range accessible by the scanning tip.

In order to characterize the thickness t of the film, we used light spectroscopy. Figure 3 shows the light transmittance of the film+substrate as a function of wavelength obtained using a UV-vis spectrometer (Ocean Optics equipped with DH-2000-BAL light source and OOIBASE32 spectrometer operating software). The thickness of the magnetic film was estimated by noting that the wavelengths λ_1 and λ_2 of two neighbor interference peaks are related by $2nt(\frac{1}{\lambda_2} - \frac{1}{\lambda_1})$

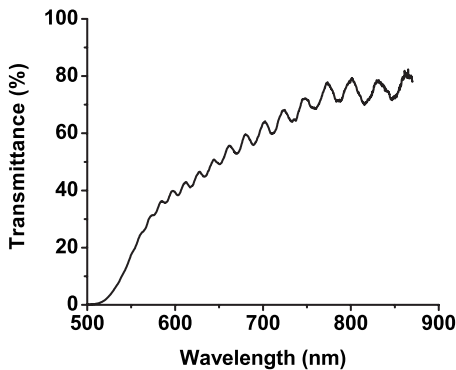
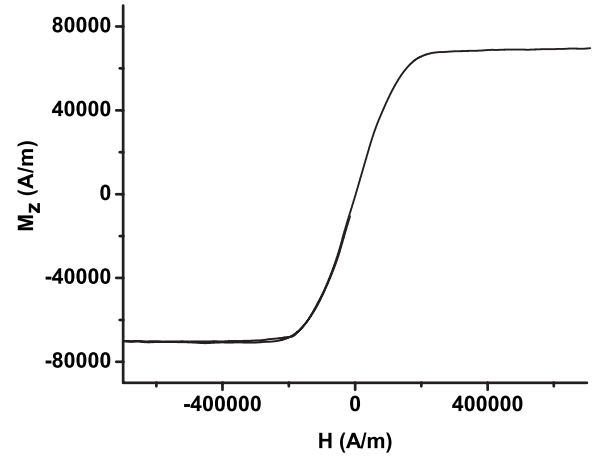


FIG. 3. Transmittance of light versus wavelength through a region far away from the crack.

FIG. 4. Magnetization M_z versus field perpendicular to the garnet film obtained using a vibrating sample magnetometer.

$= 1$, where $n \approx 2.5$ is the refractive index of the garnet film in the wavelength region of interest.⁶ By locating λ_1 and λ_2 for the peaks in the wavelength region of 650–800 nm, and then average the computed thickness, we estimated that $t = 4.0 \pm 0.5 \mu\text{m}$. The magnetization M_z perpendicular to film versus applied field was measured using a vibration sample magnetometer (Lakeshore 7404), and the results are displayed in Fig. 4. The saturation field was found to be $H_a \sim 2 \times 10^5 \text{ A/m}$, in agreement with previous reports.⁸

Quantitative magneto-optic imaging using the Kerr and Faraday effect has been extremely useful for mapping domains and domain walls.^{11,24} In the current study, the Faraday rotation of local regions of the garnet film was measured by first adjusting the polarizer and analyzer such that their polarization axes were nearly perpendicular to each other. During an experiment, the polarizer and analyzers were kept at fixed settings. If a local magnetization vector has a component perpendicular to the magnetic film, a local Faraday rotation occurs, and this results in a corresponding gray level value recorded by the digital CCD camera.¹² Since the camera had a linear intensity response in the region considered, we could convert gray level changes into the Faraday rotation. Knowing the Faraday rotation θ_F allows us to obtain the magnetization vector along the optical axis (z axis) according to the following expression:

$$\theta_F = V \frac{M_z}{M_s} t, \quad (1)$$

where V is the Verdet constant, M_s the saturation magnetization, and t is the thickness of the film. Here, we found that $V = 2^\circ \pm 0.5^\circ \mu\text{m}^{-1}$ in regions of the film far away from the cracks, in good agreement with our previous studies.^{7,8}

III. RESULTS

Using spatially resolved magneto-optical imaging, we measured the Faraday rotation near the crack. By applying a weak in-plane magnetic field (typically $< 500 \text{ A/m}$), we could reverse the polarity of the Faraday rotation across the

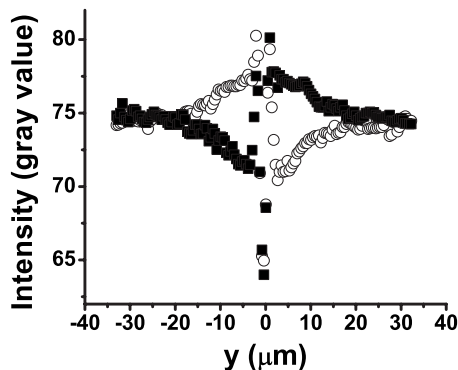


FIG. 5. The intensity distribution due to the Faraday rotation near the crack. Shown here are raw data.

crack. Since the in-plane field was weak, it did not induce a Faraday rotation in the optical components of the microscope. Two measurements of the Faraday rotation in the crack are shown in Fig. 5, where the open circles and filled squares correspond to in-plane fields of opposite polarity. Note that a few micrometers away from the crack the Faraday rotation changes sign, whereas closer to the crack, the situation is more unclear due to noise. This is due to the fact that the crack exhibits birefringence, which overlaps with the Faraday signal and therefore reduces the resolution. By subtracting the two signals of Fig. 5, we were able to reduce much of the noise closer to the crack, since the noise as well as the birefringence near the crack do not change upon applying a weak in-plane magnetic field. The squares of Fig. 6 shows the Faraday rotation as a function of position from the one-dimensional crack. The measurements represent an average over several micrometers. Despite carefully subtracting the raw signals of Fig. 5, we were not able to resolve the Faraday rotation properly at positions closer than $2 \mu\text{m}$ from the crack due to uncorrelated noise in this region. We note from Fig. 6 that M_z switches polarity across the crack, which is due to the fact that the magnetization vectors on both sides of the crack exhibit dipolar interactions which minimize the energy. It is, of course, possible that other quadratic magneto-optic effects (e.g., the Cotton-Mouton effect) are responsible for the change in direction of the polarization vector as the light propagates through the sample. However,

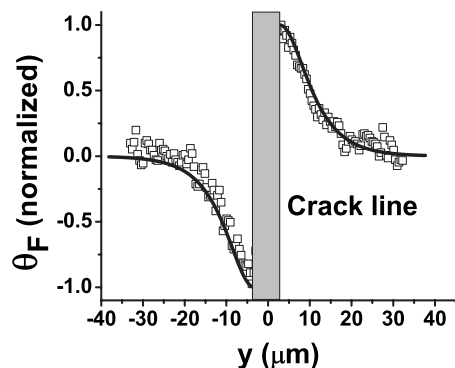


FIG. 6. The Faraday rotation associated with a domain wall near the crack.

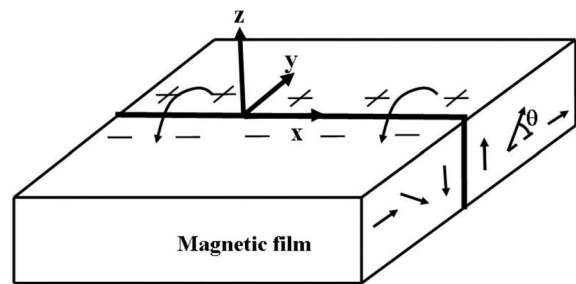


FIG. 7. Schematic drawing of the magnetization distribution near the crack. The plus or minus signs correspond to the signs of the magnetic charges on the surface of the film.

unlike the polar Faraday effect [Eq. (1)], these mechanisms depend on the angle ϕ between the in-plane magnetization vector and the electric field vector of the light beam such that the intensity is proportional to $\sin^2 2\phi$.¹⁷ To rule out these quadratic effects, we therefore rotated the sample and observed no notable changes in the magneto-optic image. We may therefore conclude that the polar Faraday effect appears to be responsible for observability of domain wall structure using a polarization microscope, and thus the magnetization is proportional to the Faraday rotation as stated in Eq. (1).

In order to understand how the Faraday rotation changes, as seen in Fig. 6, we made a simple model based on the energy contributions from uniaxial anisotropy, demagnetization, and exchange energies. The crack is located on the x axis, while the y axis is perpendicular to it and located in the film plane. Let θ be the angle the magnetization vector forms with the y axis (see Fig. 7). The uniaxial anisotropy energy is represented by $E_u = K_u \cos^2 \theta$, where a positive uniaxial anisotropy constant K_u means that the uniaxial anisotropy energy favors the alignment of the magnetization vector with a normal to the film surface. The demagnetization energy $E_d = \frac{1}{2} \mu_0 M_s^2 \sin^2 \theta$ (μ_0 is the permeability of vacuum), and it favors a magnetization vector in the plane of the film. For a uniform magnetic film, the total energy is $E_u + E_d = K_u + K_u^{eff} \sin^2 \theta$, where $K_u^{eff} = \frac{1}{2} \mu_0 M_s^2 - K_u$. It is seen that when $K_u^{eff} > 0$, energy minimization requires that the magnetization vector is lying in the plane of the film ($\theta = 0^\circ$), while when $K_u^{eff} < 0$, it is perpendicular to the film ($\theta = 90^\circ$). For films exhibiting magnetization gradients, we need to take into account the exchange energy which is determined by $A \left(\frac{\partial \theta}{\partial y} \right)^2$, where A is the exchange constant. The total energy associated with the domain wall studied here is then²⁵

$$E = \int_{-\infty}^{\infty} \left[K_u \cos^2 \theta + \frac{1}{2} \mu_0 M_s^2 \sin^2 \theta + A \left(\frac{\partial \theta}{\partial y} \right)^2 \right] dy. \quad (2)$$

In the following, we will assume that the stress σ does not vary significantly as the magnetization vector rotates. Upon minimizing the energy, integrating from y to $y \rightarrow \infty$ and assuming that $\theta = 0$ when $y \rightarrow \infty$, we find the following differential equation:

$$K_u^{eff} \sin^2 \theta = A \left(\frac{\partial \theta}{\partial y} \right)^2. \quad (3)$$

We require that $\theta(y=0) = \theta_0$, and upon solving Eq. (3), we find

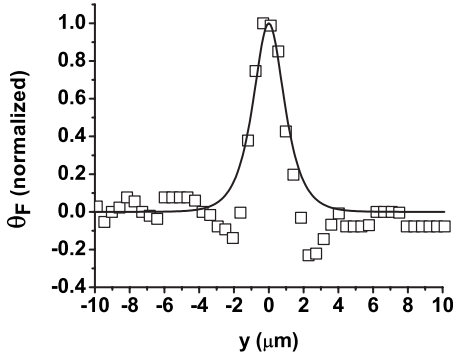


FIG. 8. The Faraday rotation associated with a Bloch wall far away from the crack.

$$\theta = 2 \tan^{-1} \left[\tan\left(\frac{\theta_0}{2}\right) \exp\left(-\sqrt{\frac{|K_u^{eff}|}{A}} y\right) \right]. \quad (4)$$

The z component of the magnetization can be found from $M_z = M_s \sin \theta$.

At $y < 0$, the magnetization direction is found to be opposite to that of $y > 0$, which is due to the fact that the system is trying to minimize its dipolar interaction energy by aligning the magnetization vectors at $y=0^-$ and $y=0^+$ antiparallel to each other. However, such dipolar interactions are often relatively short ranged,²⁵ thus only influencing the magnetization distribution at the close proximity of the crack (i.e., on the nanometer scale). Here, we are interested in the magnetization distribution on the micrometer scale and will therefore neglect dipolar interactions between domains. Under these assumptions, the magnetization distribution for $y < 0$ is found from Eq. (3) to be

$$\theta = -2 \tan^{-1} \left[\tan\left(\frac{\theta_0}{2}\right) \exp\left(\sqrt{\frac{|K_u^{eff}|}{A}} y\right) \right]. \quad (5)$$

A schematic drawing of the magnetization distribution is seen in Fig. 7. We fitted Eqs. (4) and (5) to the experimental data in Fig. 6 assuming a domain wall width $w = \sqrt{\frac{A}{|K_u^{eff}|}} = 6 \mu\text{m}$ and $\theta_0 \approx 90^\circ$. The result is displayed as two solid lines in Fig. 6, which are seen to fit well with the experimental data.

For comparison, we also recorded the magneto-optic profile of normal 180° Bloch walls, separating regions where the magnetization vector is pointing in the positive ($y > 0$) or negative ($y < 0$) y direction, located far from the cracks. Figure 8 shows the normalized Faraday rotation (after subtracting the background) associated with one of these Bloch

walls. It is well known that the z component of the magnetization vector associated with such a Bloch wall is given by $M_z = M_s \sin \theta$, where^{22,25}

$$\theta = 2 \tan^{-1} \left[\exp\left(-\sqrt{\frac{|K_u^{eff}|}{A}} y\right) \right]. \quad (6)$$

By fitting Eq. (6) to the experimental data assuming a domain wall width $w_B = \sqrt{\frac{A}{|K_u^{eff}|}} = 0.8 \mu\text{m}$, we obtained the solid line in Fig. 8. The deviations between the experimental data and our theoretical fit are attributed to diffraction, which is known to create “ringing” near the edge of the lobe. It should be noted that the Bloch wall width is much smaller than that found for the domain walls near the crack.

A plausible explanation is as follows. The garnet film studied here exhibits a small positive uniaxial anisotropy K_{u0} in the absence of stress.^{6,8} Thus, at the position of the crack where the stress has been relaxed (i.e., is small), $K_u(y \approx 0) \approx K_{u0} > 0$ and $K_u^{eff}(y \approx 0) < 0$, such that the magnetization vector is perpendicular to the magnetic film. However, further away from the crack, the stress σ plays a role, and the uniaxial anisotropy decreases according to $K_u(y) = K_{u0} + (3/2)\sigma(y)\lambda$, where $\lambda < 0$.¹⁶ Far from the crack, we found that the magnetization vector is lying in the plane of the magnetic film, which means that $K_u^{eff}(y \rightarrow \infty) > 0$. Since the domain wall close to the crack is much wider than that far away from the crack, we also know that $|K_u^{eff}(y \rightarrow \infty)| \gg |K_u^{eff}(y \approx 0)|$. From our magneto-optical images, it appears that the wall width decreases to its minimum value at distances $\geq 10 \mu\text{m}$ away from the crack, thus suggesting that our assumption of constant K_u is reasonable when deriving Eqs. (4) and (5).

IV. CONCLUSION

We have studied the domain wall structure near cracks in ferrimagnetic garnet films and shown that the magnetization vector has a vector component perpendicular to the film near the crack, but rotates to align with the film a few micrometers away. This interesting behavior is attributed to the pinning of the magnetic moment, and a model is presented to provide further insight into the rotation of the magnetization vector. The domain wall structures reported here can be used to efficiently manipulate magnetic colloids, thus allowing one to use the cracked magnetic films for micro- and nanomanipulation in microfluidic settings as well as for investigating forces between particles. Due to the ease operation of such systems, one may project that they may be particularly attractive for creating components for lab-on-a-chip.

¹M. N. Deeter, A. H. Rose, G. W. Day, and S. Samuelson, J. Appl. Phys. **70**, 6407 (1991).

²W. Tolksdorf and C. P. Klages, Thin Solid Films **114**, 33 (1984).

³R. W. Hansen, L. E. Helseth, A. Solovyev, E. I. Il'yashenko, and T. H. Johansen, J. Magn. Magn. Mater. **272-276**, 2247 (2004).

⁴I. J. Park, K. U. Kang, and C. S. Kim, IEEE Trans. Magn. **42**, 2882 (2006).

⁵I. Nistora, C. Holthaus, I. D. Mayergoyz, and C. Krafft, J. Appl. Phys. **99**, 08M702 (2006).

⁶P. Hansen, C. P. Klages, J. Schuldt, and K. Witter, Phys. Rev. B

- 31**, 5858 (1985).
- ⁷L. E. Helseth, R. W. Hansen, E. I. Il'yashenko, M. Baziljevich, and T. H. Johansen, Phys. Rev. B **64**, 174406 (2001).
- ⁸L. E. Helseth, A. G. Solov'yev, R. W. Hansen, E. I. Il'yashenko, M. Baziljevich, and T. H. Johansen, Phys. Rev. B **66**, 064405 (2002).
- ⁹G. Y. Zhang, X. W. Xu, and T. C. Chong, J. Appl. Phys. **95**, 5267 (2004).
- ¹⁰Z. C. Xu, M. Yan, M. Li, Z. L. Zhang, and M. Huang, J. Appl. Phys. **101**, 053910 (2007).
- ¹¹L. A. Dorosinskii, M. V. Indenbom, V. I. Nikitenko, Y. A. Osipyan, A. A. Polyanskii, and V. K. Vlasko-Vlasov, Physica C **203**, 149 (1992).
- ¹²M. Baziljevich, T. H. Johansen, H. Bratsberg, Y. Shen, and P. Vase, Appl. Phys. Lett. **69**, 3590 (1996).
- ¹³F. Laviano, D. Botta, A. Chiodoni, R. Gerbaldo, G. Chigo, L. Gozzelino, S. Zannella, and E. Mezzetti, Supercond. Sci. Technol. **16**, 71 (2003).
- ¹⁴H. Ferrari, V. Bekeris, and T. H. Johansen, Physica B **398**, 476 (2007).
- ¹⁵A. Shevchenko, M. Korppi, K. Lindfors, M. Heiliö, M. Kaivola, E. Il'yashenko, and T. H. Johansen, Appl. Phys. Lett. **91**, 041916 (2007).
- ¹⁶M. H. Kryder, T. J. Gallagher, and R. A. Scranton, J. Appl. Phys. **53**, 5810 (1982).
- ¹⁷B. E. Argyle and E. Terenzio, J. Appl. Phys. **55**, 2569 (1984).
- ¹⁸L. E. Helseth, R. W. Hansen, T. H. Johansen, and T. M. Fischer, Appl. Phys. Lett. **85**, 2556 (2004).
- ¹⁹L. E. Helseth and T. M. Fischer, Langmuir **20**, 8192 (2004).
- ²⁰L. E. Helseth, T. H. Johansen, and T. M. Fischer, Phys. Rev. E **71**, 062402 (2005).
- ²¹L. E. Helseth, H. Z. Wen, and T. M. Fischer, J. Appl. Phys. **99**, 024909 (2006).
- ²²A. Hubert and R. Schäfer, *Magnetic Domains: The Analysis of Magnetic Microstructures* (Springer, Berlin, 1998).
- ²³J. McCord, J. Appl. Phys. **95**, 6855 (2004).
- ²⁴W. Rave, R. Schäfer, and A. Hubert, J. Magn. Magn. Mater. **65**, 7 (1987).
- ²⁵D. Craik, *Magnetism: Principles and Applications* (Wiley, Chichester, 1995).